Noisy Inflows Cause a Shedding-Mode Switching in Flow Past an Oscillating Cylinder

Didier Lucor* and George Em Karniadakis†

Division of Applied Mathematics, Brown University, Providence, Rhode Island 02912, USA

(Received 17 December 2003; published 16 April 2004)

Vortex streets formed behind oscillating bluff bodies consist of arrays of groups of two, three, or four vortices classified as $2S$, $P+S$, and $2P$ shedding modes, respectively. The prevailing dominant mode depends primarily on the amplitude and the frequency of the oscillation and on the Reynolds number. We investigate the effect of noise at the inflow on the stability of these vortex modes in laminar flow past a circular cylinder. We employ stochastic simulations based on a new polynomial chaos method to study the shedding-mode switching from a $P+S$ pattern to a $2S$ mode in the presence of noise.

DOI: 10.1103/PhysRevLett.92.154501 PACS numbers: 47.15.Fe, 46.65.+g, 47.27.Vf

One of the main features of the flow past a cylinder oscillating transversely in a free stream is *lock-in,* a frequency synchronization phenomenon. In experimental work, the motion of the cylinder is often prescribed in order to mimic the vortex-induced oscillations of a free, i.e., elastically mounted cylinder; see [1,2], and references therein. The different synchronization regions for such prescribed cylinder oscillations have been mapped in an amplitude-wavelength plane by Williamson and Roshko [3]. The dominant vortex patterns near the fundamental synchronization region are $2S$, $2P$, and $P+S$. A $2S$ shedding mode implies that in each half-cycle of the oscillation a single vortex is shed into the wake. A $2P$ shedding mode means that in each half-cycle a pair of vortices of opposite sign is shed into the wake. Finally, a $P+S$ mode is an asymmetric version of the $2P$ mode where the cylinder sheds a pair of vortices of opposite sign and a single vortex each cycle. Adopting this classification, the standard von Kármán vortex street is equivalent to a $2S$ mode. Some vortex formation processes, such as the ones leading to $2P$ and $P+S$ shedding modes, appear to be more unstable than the $2S$ and sensitive to different experimental conditions [4,5]. More generally, the boundaries between the different regimes identified in the experiments of [3] seem not to be robust, and indeed they depend on many parameters including Reynolds number, thermal effects, turbulence level, start-up conditions, etc.

In this work, we consider the effect of noisy inflow on the vortex formation behind an oscillating circular cylinder. More specifically, we simulate stochastically laminar flow past an oscillating circular cylinder with random inflow, i.e., consisting of a uniform mean inflow plus a random component; the latter follows a *uniform* distribution. We employ a new simulation method based on generalized polynomial chaos (GPC) algorithms developed in [6,7]. This is an extension of the classical polynomial chaos that employs Wiener-Hermite expansions [8,9]. GPC represents efficiently Gaussian and non-Gaussian second-order random processes in terms of orthogonal polynomials functionals. The expansion basis $\Psi_j(\boldsymbol{\xi}(\theta))$ is a complete basis from the Askey family of polynomials [10]. Using this representation, a general second-order random process takes the form

$$u(\boldsymbol{x}, t; \theta) = \sum_{j=0}^{P} u_j(\boldsymbol{x}, t)\Psi_j(\boldsymbol{\xi}(\theta)) \quad \text{with } P = \frac{(n+p)!}{n!p!} - 1, \tag{1}$$

where n is the number of random dimensions and p is the highest polynomial order of the GPC expansion. Also, $\boldsymbol{\xi}(\theta)$ is the vector of independent random variables ξ_i, which are functions of the independent random parameter θ.

The numerical procedure involves a Galerkin projection of the Navier-Stokes equations onto the random basis $\Psi(\boldsymbol{\xi}(\theta))$. The system of equations is greatly simplified and the convergence rate is improved significantly as there exists an exact *correspondence* between the weights of the orthogonal polynomials in the Askey family and the probability functions of certain types of random distributions [10]. For instance, the optimal polynomial basis for Gaussian or uniform random processes are the Hermite or Legendre polynomials, respectively. We solve the two-dimensional incompressible Navier-Stokes equations

$$\nabla \cdot \mathbf{u} = 0, \tag{2}$$

$$\frac{\partial \mathbf{u}}{\partial t} + \mathbf{u} \cdot \nabla \mathbf{u} = -\nabla p + \mathrm{Re}^{-1}\nabla^2 \mathbf{u}, \tag{3}$$

where $\mathrm{Re} = \overline{U}d/\nu$ is the Reynolds number based on the mean inflow velocity $\overline{U}$. We first expand the velocity and pressure in terms of their GPC expansion, i.e.,

$$\mathbf{u}(\boldsymbol{x}, t, \theta) = \sum_{i=0}^{P} \boldsymbol{u}_i(\boldsymbol{x}, t)\Psi_i(\boldsymbol{\xi}(\theta)), \tag{4}$$

$$p(\boldsymbol{x}, t; \theta) = \sum_{i=0}^{P} p_i(\boldsymbol{x}, t)\Psi_i(\boldsymbol{\xi}(\theta)). \tag{5}$$

We then substitute into the Navier-Stokes equations, and subsequently we project the obtained equations onto the random space spanned by the GPC basis. That is, we take the inner product with each basis and use the orthogonality condition to simplify the equations. We obtain a discrete set of *deterministic* equations for each of the random modes, $k = 0, 1, \ldots, P$:

$$\nabla \cdot \boldsymbol{u}_k = 0$$
$$\frac{\partial \boldsymbol{u}_k}{\partial t} = -\sum_{i=0}^{P}\sum_{j=0}^{P}\frac{e_{ijk}}{\langle \Psi_k^2 \rangle}(\boldsymbol{u}_i \cdot \nabla)\boldsymbol{u}_j - \nabla p_k + \nu \nabla^2 \boldsymbol{u}_k, \tag{6}$$

where $e_{ijk} = \langle \Psi_i \Psi_j \Psi_k \rangle$. The above set of deterministic $(P + 1)$ "Navier-Stokes–like" equations for each random mode is only coupled through the convective terms. The inflow velocity takes the form of a stationary uniform random variable and is $U(\theta) = \overline{U} + \sigma_U \xi(\theta)$; $V = 0$, where ξ is a uniform random variable of zero mean and unit variance. The cylinder motion is imposed in a purely deterministic manner. The above equations are solved using a mapping approach based on a technique developed in [11]. For a two-dimensional flow, this mapping transformation amounts to an adjustment of flow velocity by the cylinder velocity, which is deterministic in our application. The transformation adds an extra forcing term to the Navier-Stokes equations, which is the cylinder acceleration in the cross-flow direction; we only assume transverse oscillations here. Discretization in space and time can be carried out by any numerical method; here we use the spectral/hp element method in space in order to have better control of the numerical error coming from the deterministic part of model [12]. The high-order splitting scheme based on consistent pressure boundary conditions is employed for time discretization [12]. In particular, the spatial discretization is based on Jacobi polynomials of order 6 employed on 708 triangular elements. With respect to resolution in random space, a convergence study showed that for a uniform distribution Legendre polynomials of order $p = 15$ are adequate for the highest noise level employed in our simulations (30%). More details of GPC and discretization along with verification studies can be found in [13].

We first simulated $\mathrm{Re} = 140$ and tested different levels of noise. The cylinder is forced to oscillate in a purely harmonic deterministic motion with amplitude $A/d = 1.0$ and reduced velocity based on the excitation frequency $V_{rn} = \overline{U}d/f_e = 7.5$. This choice of parameters leads to a $P + S$ shedding mode in deterministic simulations, i.e., in the absence of noise at the inflow. The experimental results of Williamson and Roshko [3] indicate a $2P$ mode for these conditions but at a larger Reynolds number. In our deterministic simulations, a $2P$ mode is first excited, but it switches to a $P + S$ mode after a while. At high Reynolds number previous simulations have demonstrated that the $2P$ shedding mode is the preferred flow state; see [14]. Visualizations of deterministic vorticity at different instants within one shedding cycle and spectral analysis of the cylinder forces indicate that we obtain a stable $P + S$ sheding mode. The top image in Fig. 1 shows an example of the $P + S$ shedding mode at $y/d = 0$ with one pair ($P1$) of vortices (I and II) shed from the cylinder upper side and one single ($S1$) vortex shed from the lower side.

We now present results from the stochastic simulations. The lower three images in Fig. 1 show instantaneous

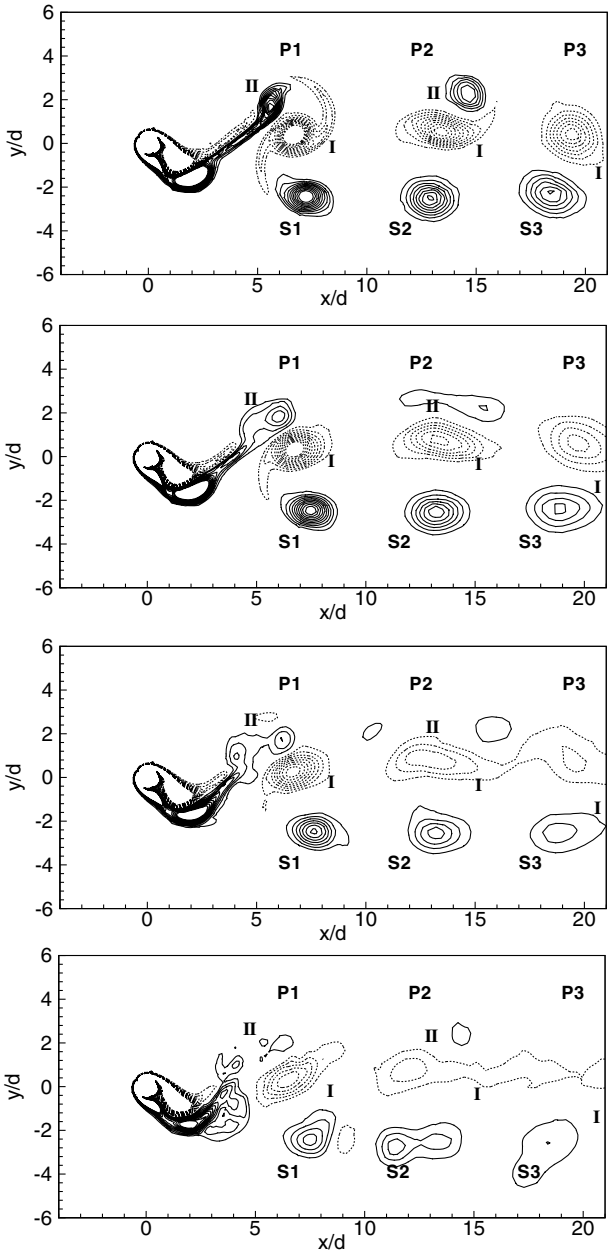

FIG. 1. Comparison between deterministic (top) and stochastic mean instantaneous vorticity fields for different levels of noise σ_U at identical time and $y/d = 0$; $\sigma_U = 10\%\ \overline{U}$ (second); $\sigma_U = 20\%\ \overline{U}$ (third); $\sigma_U = 30\%\ \overline{U}$ (bottom). $\overline{\mathrm{Re}} = 140$; $p = 15$.

stochastic mean vorticity contours (at the same time as the deterministic simulation) for different levels of noise. The location of the letters identifying the vortices do not change in the four different plots. The effect of the noise is striking; the vortex street in the wake is reorganized as the level of noise increases from 10% to 20% to 30%; see Fig. 1. These results seem to indicate that the noise affects primarily the formation of the second vortex of each pair in the $P + S$ mode; this is particularly clear in the second plot from the top. For this case, corresponding to a moderate level of noise, we see that the second vortex (II) of the first ($P1$) and second ($P2$) pairs are really affected while the other vortical structures (I of $P1$ and I of $P2$, $S1$, $S2$, $S3$) remain almost intact. We also note that the circulation of the second vortex of each pair of deterministic vortices is weaker than the first vortex. This was also observed in the case of the $2P$ shedding mode in the wake of *free* rigid cylinders in cross flow [15]. This suggests that the weakest vortical structures of the wake are the first ones to suffer the effect of noise.

Figure 2 shows a similar comparison for the case of a $P + S$ shedding mode of a forced cylinder at $\mathrm{Re} = 400$ with $A/d = 0.5$ and $V_{rn} = 6.0$. We note that, according to the experimental results in [3], a $2P$ mode should be the dominant one at Reynolds number greater than 392. It seems, however, that the $2P$ mode is not captured in a two-dimensional simulation in contrast to three-dimensional simulations [14]. In this case, due to the higher value of the Reynolds number, a smaller noise level $\sigma_U = 10\%\ \overline{U}$ is sufficient to completely alter the wake dynamics. For both Reynolds numbers we simulated, we see that a noisy inflow changes dramatically the vortex formation in the wake. As we increase the noise level, the $P + S$ mode undergoes a transformation that brings it closer to a $2S$ mode; i.e., we recover the classical shedding mode of the vortex street of a stationary cylinder.

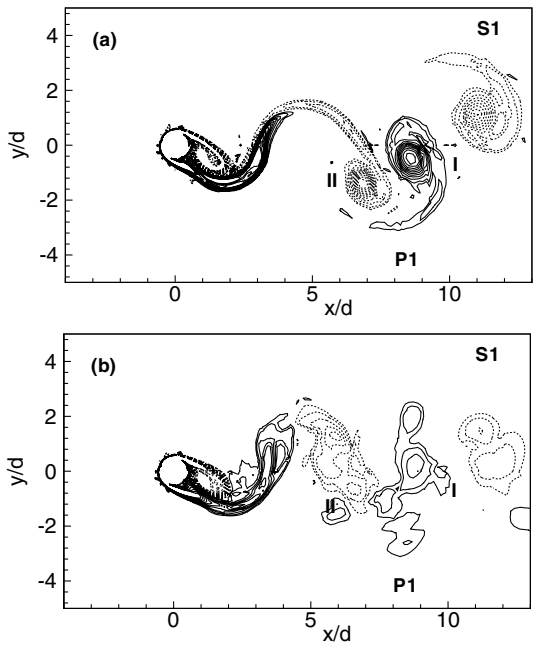

FIG. 2. Comparison between the deterministic (a) and the mean (b) instantaneous vorticity field at identical time and $y/d = 0$; $\sigma_U = 10\%\ \overline{U}$; $\overline{\mathrm{Re}} = 400$; $p = 10$.

Next, we examine the effect of noise on the cylinder forces. Figure 3(a) compares the time evolution of the deterministic and stochastic *mean* lift coefficients for different noise levels. Figure 3(b) shows the corresponding spectra of the deterministic and stochastic mean lift coefficients. We see in Fig. 3(a) that the values of the stochastic mean amplitude values of the lift force are lower than the deterministic case. A threshold in the noise level seems to exist above which the force mean values are noticeably different from the deterministic forces. Indeed, a value of $\sigma_U = 10\%\ \overline{U}$ does not affect significantly the mean solution, but $\sigma_U \geq 20\%\ \overline{U}$ does. Interestingly, the stochastic mean solutions are smoother than the deterministic solution. The additional weaker oscillation of the deterministic solution [see, for instance, Fig. 3(a) in $[-0.5; 0]$ range], symptomatic of the shedding of the pair of vortices of the $P + S$ mode, is almost completely eliminated from the mean solution with large noise intensity.

The above observation is confirmed by the spectral analysis of the lift force; see Fig. 3(b). The two loading frequencies of the deterministic forces are the Strouhal frequency corresponding to the $2S$ mode and the first superharmonic at twice this frequency corresponding to the $2P$ mode. While the energy remains constant in the first peak, there is a decrease of the energy in the second peak for the stochastic case. A purely $2S$ mode would correspond to a case where most of the energy is eliminated for the second peak and concentrates only in the

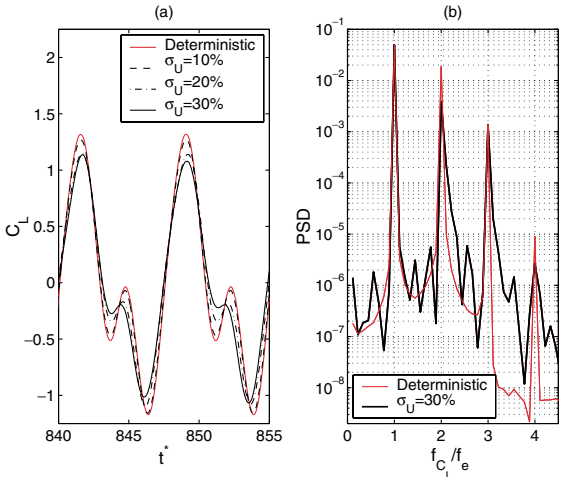

FIG. 3 (color online). Comparison between deterministic and mean lift coefficient for different levels of noise. (b) Comparison between the deterministic and the mean spectrum of lift coefficient. $\overline{\mathrm{Re}} = 140$; $p = 15$; $t^* = t\overline{U}/d$; $f_e = U/7.5d$.

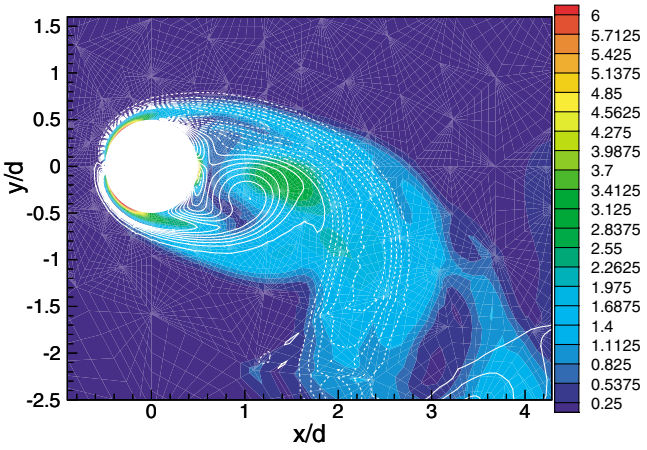

FIG. 4 (color online). Comparison of instantaneous rms values (multicolor flood) and deterministic values (white isocontour lines) of vorticity at identical time; $y/d = 1.0$. $\sigma_U = 30\%$ $\overline{U}$, $\overline{\mathrm{Re}} = 140$, and $p = 15$. Contour levels for the deterministic vorticity are $\omega d/\overline{U} = \pm 0.4, \pm 1.2, \pm 2.0, \ldots$.

first peak ($f_{C_L}/f_e = 1$). We notice that the noise affects the entire spectrum and flattens it. As we have observed in the flow visualization, the noise first affects and suppresses the formation of the second vortex of each pair of vortices in the $P + S$ mode. The vortical topology of the wake then becomes more similar to a $2S$ shedding mode as we increase the noise level.

Figure 4 shows instantaneous root-mean square (rms) (multicolor) isocontours of the stochastic vorticity field superimposed on (white-line) isocontours of the deterministic field at the same time instant. The regions of uncertainty (large rms) in the very near wake exhibit a complex distribution that seems to match to some extent the main features of the deterministic field. For instance, regions within the boundary layer, on both sides of the front stagnation point, where most of the vorticity is generated at the wall, correspond to regions of maximum uncertainty. Large uncertainty in the flow is also present in the shear layers, close to the rear stagnation point, as well as in a bubble about one diameter downstream of the body. However, there exists a region of low uncertainty between the two shear layers and this bubble. This was also noticed at other times. The regions of uncertainty are representative of the local flow features that are affected mostly by the presence of noise introduced at the inflow.

Mode switching for the setup we consider here has also been observed experimentally. For example, in [5] a switch from a $2P$ pattern to a $2S$ pattern was observed and attributed to the start-up conditions. In [4] temperature variations caused a fluctuation of viscosity of up to 20% in the wake resulting also in mode switching from a $2P$ to a $2S$ pattern although this transition was back and forth and not a one-time event. These results are consistent with the present findings, but a careful experimental study with controlled random disturbances at the inflow is required to validate the exact findings of our simulation work.

This work was supported by the ONR and AFOSR, and computations were performed on the DoD supercomputing facilities at ERDC/NAVO.

*Electronic address: didi@dam.brown.edu
†Electronic address: gk@dam.brown.edu

[1] A. Ongoren and D. Rockwell, J. Fluid Mech. **191**, 197 (1988).
[2] O. Griffin and S. Ramberg, J. Fluid Mech. **66**, 553 (1974).
[3] C. Williamson and A. Roshko, J. Fluids Struct. **2**, 355 (1988).
[4] T. Pottebaum, Ph.D. thesis, California Institute of Technology, 2003.
[5] J. Carberry, J. Sheridan, and D. Rockwell, J. Fluids Struct. **15**, 523 (2001).
[6] D. Xiu, D. Lucor, C.-H. Su, and G. Karniadakis, J. Fluids Eng. **124**, 51 (2002).
[7] D. Lucor, D. Xiu, C.-H. Su, and G. Karniadakis, Int. J. Numer. Methods Fluids **43**, 483 (2003).
[8] N. Wiener, Am. J. Math. **60**, 897 (1938).
[9] R. Ghanem and P. Spanos, *Stochastic Finite Elements: A Spectral Approach* (Springer-Verlag, Berlin, 1991).
[10] D. Xiu and G. Karniadakis, SIAM J. Sci. Comput. **24**, 619 (2002).
[11] D. Newman and G. Karniadakis, J. Fluid Mech. **344**, 95 (1997).
[12] G. Karniadakis and S. Sherwin, *Spectral/hp Element Methods in CFD* (Oxford University Press, New York, 1999).
[13] D. Lucor, Ph.D. thesis, Brown University, 2004.
[14] C. Evangelinos and G. Karniadakis, J. Fluid Mech. **400**, 91 (1999).
[15] R. Govardhan and C. Williamson, J. Fluid Mech. **420**, 85 (2000).